



LAWRENCE
LIVERMORE
NATIONAL
LABORATORY

Unusual emission lines of carbon in the 170-190 Å region on NSTX

J. K. Lepson, P. Beiersdorfer, M. Bitter, A. L.
Roquemore, R. Kaita

February 19, 2014

Atomic Processes in Plasmas
Auburn, AL, United States
October 7, 2013 through October 10, 2013

Disclaimer

This document was prepared as an account of work sponsored by an agency of the United States government. Neither the United States government nor Lawrence Livermore National Security, LLC, nor any of their employees makes any warranty, expressed or implied, or assumes any legal liability or responsibility for the accuracy, completeness, or usefulness of any information, apparatus, product, or process disclosed, or represents that its use would not infringe privately owned rights. Reference herein to any specific commercial product, process, or service by trade name, trademark, manufacturer, or otherwise does not necessarily constitute or imply its endorsement, recommendation, or favoring by the United States government or Lawrence Livermore National Security, LLC. The views and opinions of authors expressed herein do not necessarily state or reflect those of the United States government or Lawrence Livermore National Security, LLC, and shall not be used for advertising or product endorsement purposes.

Unusual emission lines of carbon in the 170-190 Å region on NSTX

J. K. Lepson*, P. Beiersdorfer[†], M. Bitter**, A. L. Roquemore** and R. Kaita**

**Space Sciences Laboratory, University of California, Berkeley, CA 94720 USA*

[†]*Physics Department, Lawrence Livermore National Laboratory, Livermore, CA 94550, USA*

***Princeton Plasma Physics Laboratory, Princeton, NJ 08543, USA*

Abstract.

We measured the spectral emission of plasmas from the National Spherical Tokamak Experiment in the extreme ultraviolet region, typically dominated by M-shell iron lines. Although we found that most of the significant emission in the 170–270 Å region emanates from iron, there are also some strong lines of carbon present. We show that the carbon lines are not produced by electron-impact excitation, and we speculate that they are formed instead by charge exchange.

Keywords: atomic processes – line: identification – techniques: spectroscopic

PACS: 32.30.Jc, 52.25.Vy, 52.55.Fa, 52.70.-m

INTRODUCTION

Charge exchange is an important process in astrophysics. Charge exchange occurs extensively in the solar system, e.g., in the interaction of neutral atoms of cometary comae and planetary atmospheres with the highly charged solar wind [1, 2, 3, 4]. It may also be a significant source of soft x rays in such objects as supernova remnants and starburst galaxies [5, 6]. Charge exchange is also known to occur in a variety of such terrestrial plasmas, such as tokamaks [7, 8, 9].

The search for astrophysical charge exchange phenomena has so far mainly focused on the x-ray emission of K-shell ions [1, 10, 11] because of the available detection systems currently in orbit. Identifying lines produced by charge exchange in other spectral bands may accelerate the search for this cosmic line formation process. The extreme ultraviolet region is of particular interest because both the *Chandra* and *XMM-Newton* x-ray observatories are sensitive to emission in this region from cosmic sources. Moreover, the *Hinode* satellite and the *Solar Dynamics Observatory* observe this spectral band in the sun.

In the following, we report on lines of carbon in the 170–215 Å region that cannot be explained by collisional excitation. Based on concurrent measurements of the C V and C VI K-shell emission lines, we suggest that these are produced by charge exchange.

METHODS

We obtained time-resolved spectra on NSTX using the time-resolving Long-Wavelength EUV Spectrometer (LoWEUS) instrument [12]. LoWEUS is a flat-field grating spectrometer with variable line spacing and a mean 1200 ℓ/mm , based on a design originally used at the Livermore electron beam ion trap [13, 14]. The spectral resolution is ~ 0.3 Å, resulting in a resolving power $\lambda/\Delta\lambda \sim 500$ –800 in the 150–250 Å region we examined. LoWEUS had a time resolution of ~ 13 ms at the time (since then upgraded to ~ 5 ms [15]), enabling examination of impurity evolution over the duration of the shot, as well as better correlation of emission with plasma conditions as measured by multi-point Thomson scattering (e.g., Fig. 1 in [15]). Our group has also installed similar instruments on the Alcator tokamak [16, 17].

The iron emission observed in this region was compared to modeling calculations using the CHIANTI database (v. 7.0 [18, 19]). Good agreement was found, similar to that reported in [20, 21], and we do not repeat such fits here. Calculations of the carbon line emission from collisional excitation were performed using the Flexible Atomic Code [22]. The line emission was calculated for the temperature of maximum abundance for C V (31 eV) and C VI (87 eV),

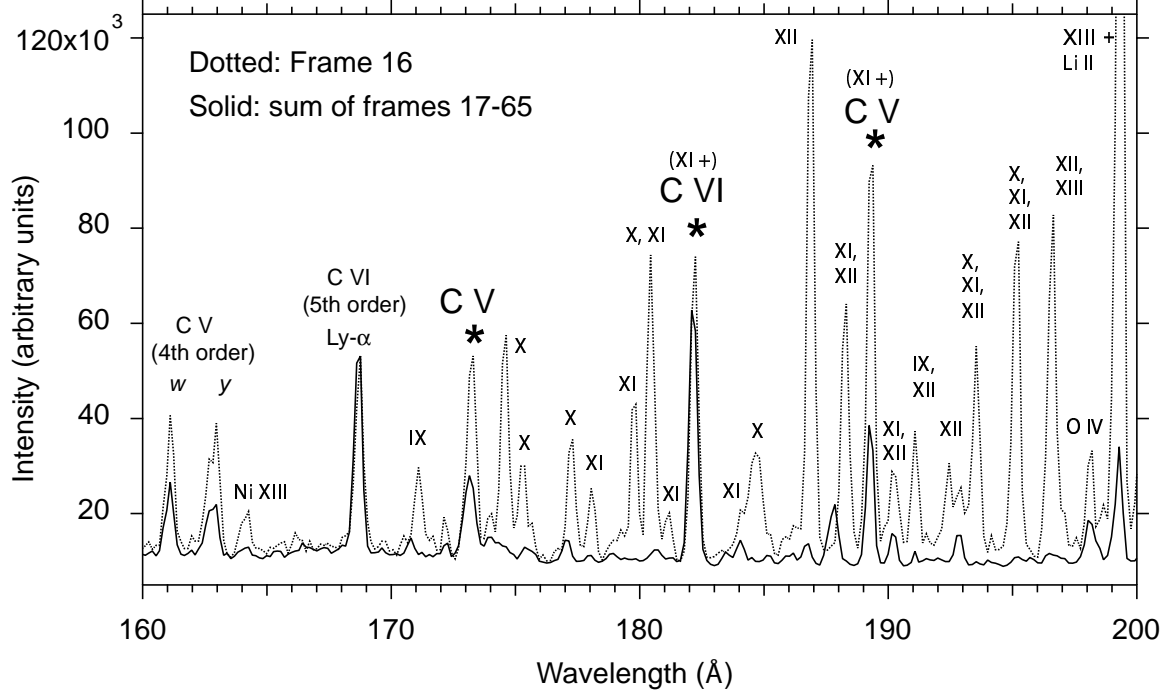


FIGURE 1. Spectrum of NSTX Shot 14111 taken by LoWEUS at different times. Strongest iron lines are identified by charge state. Dotted line: ~ 200 ms into the shot. Strong, non-iron features are indicated by asterisks associated with CV and C VI. Solid line: summation of the temporal emission of the remainder of shot (40 frames, ~ 220 – 800 ms). The roman numerals denote the spectral number of iron forming a given peak.

using an electron density $N_e = 5 \times 10^{13} \text{cm}^{-3}$. Calculations at higher and lower densities were also performed, but no effect of density on the relative line emission could be seen.

RESULTS

We present data from NSTX shot 141111, taken on 16 Sept 2010. Iron and, to a lesser extent, nickel are present as impurities in some shots that may be due to sputtering of stainless steel components in the tokamak vessel. M-shell iron emission, when present, occurs during the beginning of the shot, typically in the first 10–100 ms, when the electron temperature of the plasma is ~ 100 – 300 eV. Shot 141111 unexpectedly included a second iron emission period ~ 170 – 220 ms into the shot, when T_e reached 500–750 eV. In Fig. 1, we show emission from ~ 200 ms into the shot, when $T_e \sim 750$ eV and $N_e \sim 4 \times 10^{13} \text{cm}^{-3}$, overlaid with emission from the remainder of the shot. The remainder of the shot, which represents the sum of the emission between 220 and 800 ms, displays very little iron emission.

Figure 2 (a) shows the full view of the spectrum in Fig. 1, together with the calculated emission of C V under collisional excitation overlaid. The calculations show the helium-like lines commonly known as w and y in 1st order, while the spectrum has these lines in 3rd and 4th order. Line intensities were normalized by using the strength of w and y in 3rd order compared to 1st order. For this, a measurement of the grating efficiency for measuring the carbon line in different orders was made at the EBIT-I machine [23] at Lawrence Livermore National Laboratory (not shown).

DISCUSSION

All significant iron emission in the NSTX plasma observed by LoWEUS, ranging from Fe VIII through Fe XV, could be identified with the CHIANTI atomic database, in accordance with earlier such analyses [20, 21]. The iron M-shell emission typically ceases to be visible after 100 ms into the discharge, when $T_e > 500$ eV. The lack of iron M-shell emission after this time can be attributed to the fact that the observable ionization balance favors L-shell iron ions, i.e.

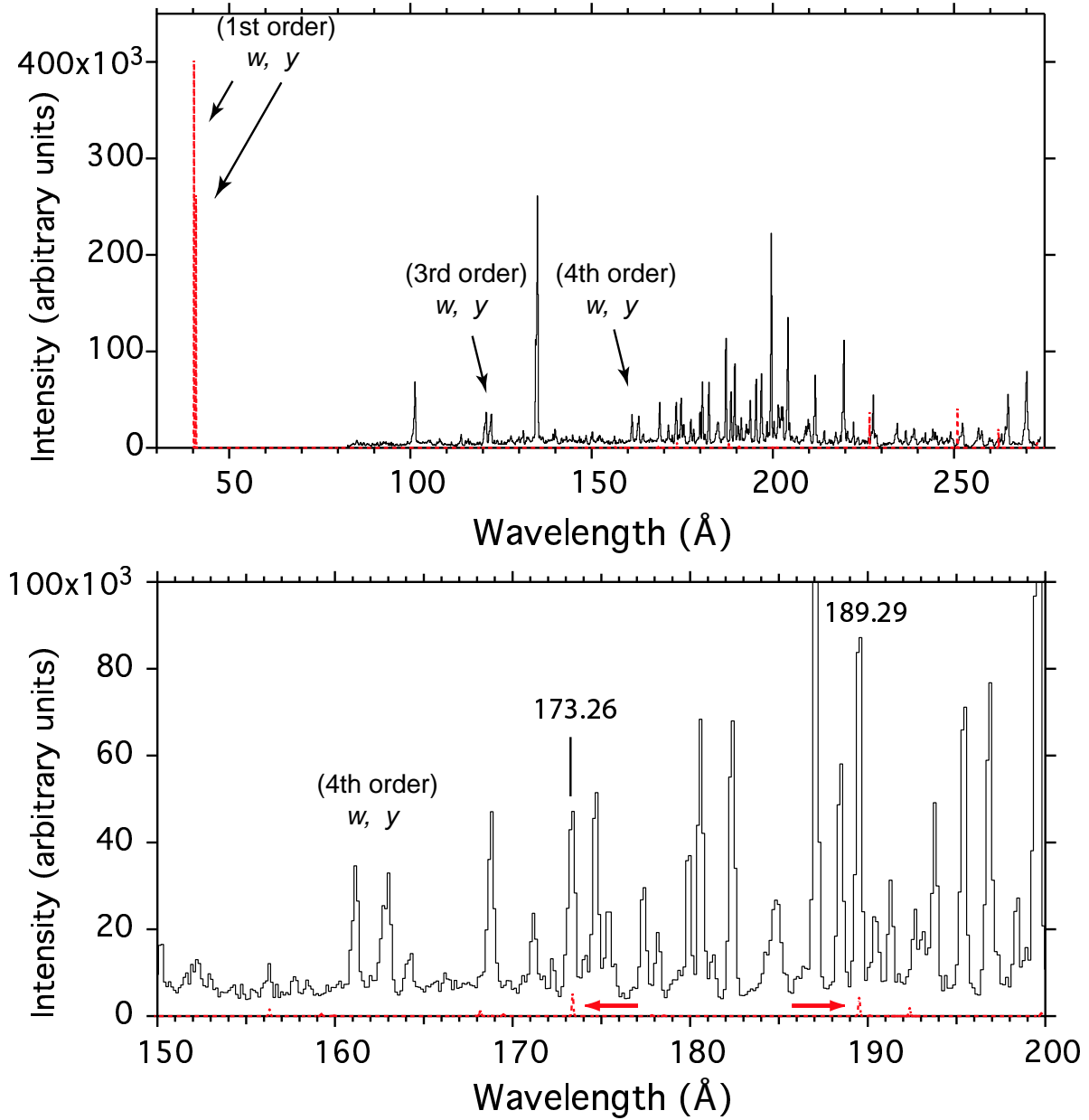


FIGURE 2. Emission of helium-like C V from collisional excitation, as calculated with the Flexible Atomic Code (dashed line), overlaid onto the LoWEUS spectrum of NSTX (solid line). Line intensities were calibrated by using the strength of lines *w* and *y* observed in 3rd order as compared to 1st order measured with EBIT-I. (top) Full spectrum, showing lines *w* and *y* in 1st order (calculated) and 3rd order (measured). (bottom) inset showing calculated vs. measured lines. Two strongest calculated lines are marked with arrows. Color version online.

Fe XVIII – Fe XXIV, which emit at lower wavelengths than covered by LoWEUS, and to a dearth of new iron influx from the vessel wall. Resumption of iron M-shell emission in this shot is attributed to an influx of cold iron from the plasma edge, probably from plasma striking the wall or an in-vessel hardware component.

Several strong features appear at this time (marked by asterisks in Fig. 1), which we have identified as emission of C V and C VI [24]. The newly observed carbon emission lines were not present in the CHIANTI astrophysical spectral database, but lines at the appropriate position were found in either the NIST (v4, [25]) or Kelly [26] databases. Support for the hypothesis that these lines are emitted by carbon is also seen in Fig. 1, which overlays the emission

at ~ 200 ms (dotted line) with emission of the remainder of the shot (~ 220 – 800 ms, solid line). Relative intensities of the new lines closely track those of the well known K-shell line of C V and C VI, which appear in higher order in the LoWEUS spectra.

These new emission lines of carbon are unlikely to be due to collisional excitation. Their strengths, calculated in our FAC models based on electron-impact excitation and seen in Fig. 2, are vanishingly small. Their absence from CHIANTI is therefore not surprising because CHIANTI relies on collisional excitation to form the lines in its data set.

We propose that the strength of the new C V and C VI lines in our spectrum are indicative of non-equilibrium processes. In particular, charge exchange of highly charged carbon with neutral hydrogen is a likely candidate process.

Charge exchange populates preferentially levels with principal quantum number n_c given by $n_c \approx q^{3/4}$ where q is the charge of the capturing ion (c.f. review by Wargelin et al. [27]). For C^{5+} and C^{6+} ions we have $n_c = 3.3$ and $n_c = 3.8$, respectively. Thus, this process mainly affects the population of the $n = 3$ and $n = 4$ levels in carbon, and our strongest lines, at 173.19 and 189.40 Å are both $4 \rightarrow 2$ transitions, while the feature at 182.23 Å is a blend of $3 \rightarrow 2$ transitions. Neutral deuterium was injected into the plasma in form of energetic beams for core plasma heating when these lines were seen. In addition, neutrals enter the plasma as recycled deuterium along the vessel wall. For example, charge exchange between helium-like Ar XVII and neutral hydrogen has been observed in the x ray region near the vessel wall at the Alcator tokamak [28].

Collisional excitation preferentially populates the singlet level so that line w is almost twice the strength of line y , whereas charge exchange preferentially populates the triplet levels so that line y is as strong or stronger than line w [9, 27]. (Note that line z is populationally de-excited, adding to the intensity of y , and it is not seen at the densities found in NSTX.) The relative strengths of the C V line pair w and y seen here (c.f. Fig. 2 bottom, where the lines are seen in 4th order) are in line with being produced in part by charge exchange and, thus, are diagnostic of charge exchange. Calculations of charge exchange in helium-like and hydrogenic carbon are ongoing and will be presented in future work.

ACKNOWLEDGMENTS

This work was supported by the DOE General Plasma Science program. Work was performed by Lawrence Livermore National Laboratory and Princeton Plasma Physics Laboratory under the auspices of the U. S. Department of Energy under Contracts DEAC52-07NA27344 and DE-AC02-09CH11466. CHIANTI is a collaborative project involving George Mason University, the University of Michigan (USA) and the University of Cambridge (UK).

REFERENCES

1. Cravens, T. E. 2002, *Science*, **296**, 1042
2. Dennerl, K. 2002, *Astron.Astrophys.*, **394**, 1119.
3. Beiersdorfer, P., Boyce, K. R., Brown, G. V., Chen, H., Kahn, S. M., Kelley, R. L., May, M., Olson, R. E., Porter, F. S., Stahle, C. K., & Tillotson, W. A. 2003, *Science*, **300**, 1558.
4. Wargelin, B. J., Markevitch, M., Juda, M., Kharchenko, V., Edgar, R., & Dalgarno, A. 2004, *Astrophys.J.*, **607**, 596.
5. Katsuda, S., Tsunemi, H., Mori, K., Uchida, H., Kosugi, H., Kimura, M., Nakajima, H., Takakura, S., Petre, R., Hewitt, J. W., & Yamaguchi, H. 2011, *Astrophys.J.*, **730**, 24.
6. Wang, Q. D., & Liu, J. 2012, *Astron.Nachrichten*, **33**, 373.
7. Källne, E., Källne, J., Dalgarno, A., Marmar, E. S., Rice, J. E., & Pradhan, A. K. 1984, *Phys.Rev.Lett.*, **52**, 2245
8. Rice, J. E., Marmar, E. S., Terry, J. L., Källne, E., & Källne, J. 1986, *Phys.Rev.Lett.*, **56**, 50.
9. Beiersdorfer, P., Bitter, M., Marion, M., & Olson, R. E. 2005, *PhysRevA*, **72**, 032725.
10. Beiersdorfer, P., Lisse, C. M., Olson, R. E., Brown, G. V., & Chen, H. 2001, *Astrophys.J.Lett.*, **549**, L147
11. Ewing, I., Christian, D. J., Bodewits, D., Dennerl, K., Lisse, C. M., & Wolk, S. J. 2012, *Astrophys.J.*, **763**, 66.
12. Lepson, J. K., Beiersdorfer, P., Clementson, J., Gu, M. F., Bitter, M., Roquemore, L., Kaita, R., Cox, P. G., & Safronova, A. S. 2010, *J.Phys.B*, **43**, 142010.
13. Beiersdorfer, P., Crespo López-Urrutia, J. R., Springer, P., Utter, S. B. & Wong, K. L. 1999, *Rev.Sci.Instrum.*, **70**, 276.
14. Graf, A., Brockington, S., Horton, R., Howard, S., Hwang, D., Beiersdorfer, P., Clementson, J., Hill, D., May, M., Mclean, H., Wood, R., Bitter, M., Terry, J., Rowan, W. L., Lepson, J. K., & Delgado-Aparicio, L. 2008, *Can.J.Phys.*, **86**, 307.
15. Lepson, J. K., Beiersdorfer, P., Bitter, M., Roquemore, L., Hill, K. W., Kaita, R., Skinner, C. H., & Zimmer, G. 2012, *Rev.Sci.Instrum.*, **83**, 10D520.
16. Reinke, M. L., Beiersdorfer, P., Howard, N. T., Magee, E. W., Podpaly, Y., Rice, J. E., & Terry, J. L. 2010, *Rev.Sci.Instrum.*, **81**, 10D736.

17. Beiersdorfer, P., Brown, G. V., Kamp, J. B., Magee, E. W., Lepson, J. K., Podpaly, Y., & Reinke, M. L. 2011, *Can.J.Phys.*, **89**, 653.
18. Dere, K. P., Landi, E., Mason, H. E., Monsignori Fossi, B. C., & Young, P. R. 1997, *Astron.Astrophys.Suppl.*, **125**, 149.
19. Landi, E., Del Zanna, G., Young, P. R., Dere, K. P. & Mason, H. E. 2012, *Astrophys.J.*, **S744**, 99.
20. Lepson, J. K., Beiersdorfer, P., Hurwitz, M., Sirk, M. M., Kato, T., & Yamamoto, N. 2008, *J.Phys.Conf.Series* **130**, 012014.
21. Beiersdorfer, P., & Lepson, J. K. 2012, *Astrophys.J.Suppl.*, **201**, 28.
22. Gu, M. F. 2008, *Can.J.Phys.*, **86**, 675.
23. Beiersdorfer, P. 2008, *Can.J.Phys.*, **86**, 1.
24. Lepson, J. K., Beiersdorfer, P., Bitter, M., Roquemore, A. L., & Kaita, R. 2013, *Phys.Scripta*, **T156**, 014075.
25. Ralchenko, Yu., Kramida, A., Reader, J. & NIST ASD Team. 2011, *NISTAtomicSpectralDatabase* (version4.1), [Online]. Available: url=<http://physics.nist.gov/asd>, National Institute of Standards and Technology, Gaithersburg, MD.
26. Kelly, R. L. 1987, *J.Phys.Chem.Ref.Data* **16**, Suppl. 1, 1.
27. Wargelin, B. J., Beiersdorfer, P., Brown, G. V. 2008, *Can.J.Phys.*, **86**, 151.
28. Rice, J. E., Marmar, E. S., Källne, E., & Källne, J. 1987, *PhysRevA*, **35**, 3033.